

Quenched disorder in the contact process on bipartite sublattices

M. N. Gonzaga¹, C. E. Fiore² and M. M. de Oliveira¹

¹*Departamento de Física e Matemática, CAP, Universidade Federal de São João del Rei, Ouro Branco-MG, 36420-000 Brazil,*

²*Instituto de Física, Universidade de São Paulo, São Paulo-SP, 05314-970, Brazil*

We study the effects of distinct types of quenched disorder in the contact process (CP) with a competitive dynamics on bipartite sublattices. In the model, the particle creation depends on its first and second neighbors and the extinction increases according to the local density. The clean (without disorder) model exhibits three phases: inactive (absorbing), active symmetric and active asymmetric, where the latter exhibits distinct sublattice densities. These phases are separated by continuous transitions; the phase diagram is reentrant. By performing mean field analysis and Monte Carlo simulations we show that symmetric disorder destroys the sublattice ordering and therefore the active asymmetric phase is not present. On the other hand, for asymmetric disorder (each sublattice presenting a distinct dilution rate) the phase transition occurs between the absorbing and the active asymmetric phases. The universality class of this transition is governed by the less disordered sublattice.

PACS numbers: 05.50.+q, 05.70.Ln, 05.70.Jk, 02.50.Ey

Keywords: Contact process, disordered systems, symmetry-breaking, absorbing state, nonequilibrium phase transitions

I. INTRODUCTION

In nonequilibrium systems, an absorbing-state phase transition occurs when a control parameter such as a creation or annihilation rate is varied, and the system undergoes a phase transition from a fluctuating state to a frozen state, with no fluctuations (the “absorbing” state). Absorbing-state phase transitions have attracted considerable interest in recent years since they are related to the description of several phenomena such as population dynamics, epidemic spreading, chemical reactions, and others [1–4]. During the last decade, several experimental realizations, e.g., in turbulent liquid crystals [5], driven suspensions [6], superconducting vortices [7] and open quantum systems [8] have highlighted the importance of this kind of phase transition.

In analogy with equilibrium phase transitions [9], it is expected that the critical phase transitions into absorbing states belong to a finite number of universality classes [4]. However, a complete classification of these nonequilibrium classes is still lacking. In general, absorbing-state transitions in models with short-range interactions and lacking a conserved quantity or symmetry beyond translational invariance belong to the directed percolation (DP) universality class [10]. On the other hand, models presenting two absorbing states linked by particle-hole symmetry are known fall in the voter model universality class [11]. There are also models that are free of absorbing states but cannot achieve thermal equilibrium because their transition rates violate the detailed balance. An example is the majority vote model [12]. In its ordered phase a Z_2 symmetry is spontaneously broken, leading to Ising-like behavior for spatial dimensions $d \geq 2$.

A few years ago, a spatially structured model that suffers a phase transition to a single absorbing state and also exhibit a broken-symmetry phase was proposed [13].

The model is based in a contact process (CP), where, besides the standard particle creation and annihilation dynamics, one includes a creation between second neighbors sites and an annihilation proportional to the local density. This results, in addition to the usual absorbing and active (symmetric) phases, in an unusual active asymmetric phase in which the distinct sublattices are unequally populated. A spontaneous symmetry breaking characterizes the reentrant phase transition between the symmetric and asymmetric phases. Mean-field theory (MFT) and simulations revealed the absorbing phase transition belongs to the directed percolation (DP) class, whereas the transitions between active phases fall into the Ising universality class, as expected from symmetry considerations. The symmetry-breaking phase transition was proven to be robust for different sublattice interactions [14] and low diffusion particle rates [15].

The inclusion of disorder can affect the critical behavior of nonequilibrium phase transitions dramatically. In real systems, quenched disorder is observed in the form of impurities and defects [16], whereas in a regular lattice it can be included in the forms of random deletion of sites or bonds [17–19] or random spatial variation of the control parameter [20, 21]. According to the Harris’ criterion [22], quenched disorder is a relevant perturbation, from the field-theoretical point of view, if $d\nu_\perp < 2$, where d is the dimensionality and ν_\perp is the correlation length exponent of the pure model. In these cases, quenched uncorrelated randomness induces the emergence of rare regions, typically located $\lambda_c(0) < \lambda < \lambda_c$, the $\lambda_c(0)$ and λ_c being the critical point for the pure and disorder models, respectively. Although globally the whole system is constrained in the subcritical phase, local supercritical regions emerge due to the presence of the disorder. The lifetime of such “active rare regions” grows exponentially with the domain size, usually leading to a slow dynamics, characterized for nonuniversal exponents toward the extinction for some interval of the control parameter below

criticality. This behavior characterizes a Griffiths phase (GP), and was verified in DP models with uncorrelated disorder irrespective to the disorder strength [23, 24]. In addition, it was shown this behavior corresponds to the universality class of the random transverse Ising model [23, 24]. However, some kinds of correlated disorder do not alter the critical behavior [25–27].

In this work, we provide a step further by investigating the effects of quenched disorder in the phase diagram of the contact processes on sublattices. Following the Harris’ criterium, disorder should be relevant for the absorbing phase transition, since $\nu_{\perp} = 0.734(4)$, for $d = 2$ in the clean system [23]. On the other hand, for the symmetry breaking phase transition, the Harris criterion is inconclusive, because it corresponds to a marginal case ($\nu = 1$ for the pure Ising model in $d = 2$) [28]. Here, we study distinct kinds of disorder, (i) a random homogeneous (ii) inhomogeneous deletion of sites, in which the disorder strength is different in each sublattice. Interesting, we show, through mean-field analysis and Monte Carlo simulations, that each one of the above disorder prescriptions yields completely different outcomes.

The remainder of this paper is organized as follows. In the next section we review the model and analyze its mean-field theory. In Sec. III we present and discuss our simulation results; Sec. IV is to summarize our conclusions.

II. MODEL AND MEAN-FIELD THEORY

Consider a stochastic interacting particle system, defined on a square lattice of linear size L , where each site can be either occupied by a particle or empty. Each particle creates a new particle in one of its first-neighbor sites with rate λ_1 , and in one of its second-neighbor sites with rate λ_2 . Note that in such *bipartite* sublattice, λ_1 is the creation rate in the opposite sublattice, whereas λ_2 is the rate in the same sublattice as the replicating particle. Therefore, *unequal* sublattice occupancies are favored if $\lambda_2 > \lambda_1$. An occupied site is emptied at a rate of unity (independent of its neighboring sites). In addition to the intrinsic annihilation rate of unity, an “inhibition term” proportional to the local density is included in the dynamics. As a consequence of this term, if the occupation fraction ρ_A of sublattice A is much larger than that of sublattice B , for instance, then any particles created in sublattice B will die out quickly, stabilizing the unequal sublattice occupancies.

In order to typify the model properties, we evaluate the macroscopic particle densities of each sublattice A and B given by ρ_A and ρ_B , respectively. In the absorbing (AB) and active symmetric (AS) phases, $\rho_A = \rho_B = 0$ and $\rho_A = \rho_B \neq 0$, respectively. Hence, $\rho = \rho_A + \rho_B$ is a reliable order parameter for absorbing phase transitions. Conversely, for the active asymmetric (AA) phase, it is convenient to calculate the difference of sublattice occupation by $\phi = |\rho_A - \rho_B|$, since ϕ distinguishes from the

AS phase, where $\phi = 0$.

The disorder is introduced by means of a fraction Γ of random deletion of sites. We shall consider two cases: the symmetric and asymmetric, in which the sublattice removal is equal ($\Gamma_A = \Gamma_B$) and different ($\Gamma_A \neq \Gamma_B$), respectively. In both cases, the disorder is quenched in space and time, i.e, its position or strength does not change during the evolution of the process. In order to achieve a qualitative portrait of the phase diagram, we begin by employing the one-site mean-field theory (MFT). For a lattice with coordination number q , it results in following coupled equations

$$\frac{d\rho_A}{dt} = -[1 + \mu q^2 \rho_B^2] \rho_A + (\lambda_1 \rho_B + \lambda_2 \rho_A)(1 - \Gamma_A - \rho_A) \quad (1)$$

and

$$\frac{d\rho_B}{dt} = -[1 + \mu q^2 \rho_A^2] \rho_B + (\lambda_1 \rho_A + \lambda_2 \rho_B)(1 - \Gamma_B - \rho_B). \quad (2)$$

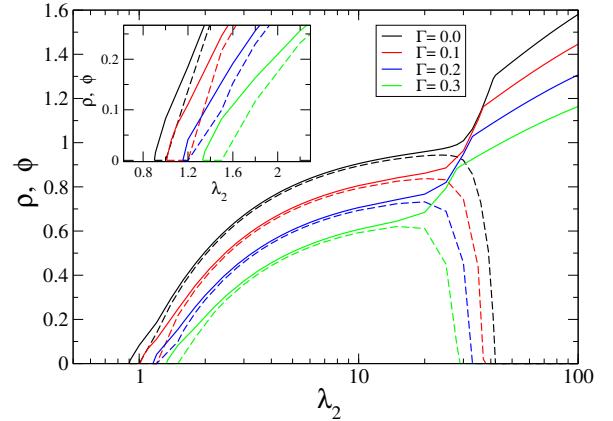


FIG. 1: (Color online) Mean-field densities ϕ (solid curves) e ρ (dahsed) for $\lambda_1 = 0.1$ and $\mu = 2.0$. Inset: detail of the data close to the absorbing transition (linear scale).

Let us first consider that the disorder is homogeneously distributed in both sublattices, i.e., $\Gamma_A = \Gamma_B = \Gamma$. In this case, one derives explicit solutions for the densities as

$$\rho = \frac{1}{2k} \left[\sqrt{\left(\frac{\lambda_1 + \lambda_2}{2}\right)^2 + 4k[(\lambda_1 + \lambda_2)(1 - \Gamma) - 1]} - \frac{\lambda_1 + \lambda_2}{2} \right] \quad (3)$$

and

$$\phi = \sqrt{\frac{-(\lambda_2 - \lambda_1)(1 - \Gamma) - 1 - \lambda_2 \rho - k \rho^2}{k}}. \quad (4)$$

The mean-field densities ρ and ϕ , are plotted as function of λ_2 , for distinct values of disorder and fixed $\lambda_1 = 0.1$ in Fig.1. For all fractions of disorder, the system undergoes a phase transition to the absorbing state at the threshold $\lambda_2 = \lambda_{2,c}^{ABS}(\Gamma)$, with $\rho = 0$, to the active symmetric phase, where $\rho > 0$ and $\phi = 0$. Note the phase transition moves for larger values of λ_2 when increasing the disorder, as expected. A further increase of λ_2 gives rise to the AS-AA and AA-AS phase transitions at $\lambda_2 = \lambda_{2,c}^I(\Gamma)$ and $\lambda_2 = \lambda_{2,c}^{II}(\Gamma)$, respectively.

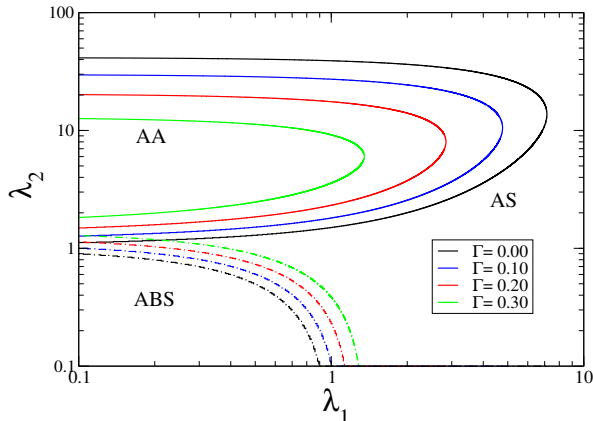


FIG. 2: Phase diagram in the $\lambda_1 - \lambda_2$ plane for $\mu = 2$, showing absorbing (ABS), active-symmetric (AS) and active asymmetric (AA) phase, for distinct values of disorder Γ .

The phase diagram for distinct values of Γ is shown in Fig. 2. The increase of Γ enlarges the absorbing phase and then the AB-AS phase transition moves for larger values of $\lambda_{2,c}^{ABS}$. In the active phase, the phase diagram is reentrant, and we note the size of the AA phase is reduced when the disorder increases.

The asymmetric disorder case, $\Gamma_A \neq \Gamma_B$, is shown in Fig. 3. MFT indicates the suppression of the AS phase, signed by a smooth change of both of ρ and ϕ at the same $\lambda_{2,c}$. The AS phase is not stable for any value of λ_2 , so that ϕ does not vanish for finite values of λ_2 . So, the phase diagram only presents two phases: the absorbing phase and the active symmetric phase separated by a continuous phase transition.

In the next section, we compare the results from MFT with those evaluated from numerical simulations.

III. RESULTS AND DISCUSSION

A. Methods

We performed extensive Monte Carlo simulations of the model on square lattices with periodic boundaries. The simulation scheme is as follows. First, a site is selected at random. If the site is occupied, it creates a

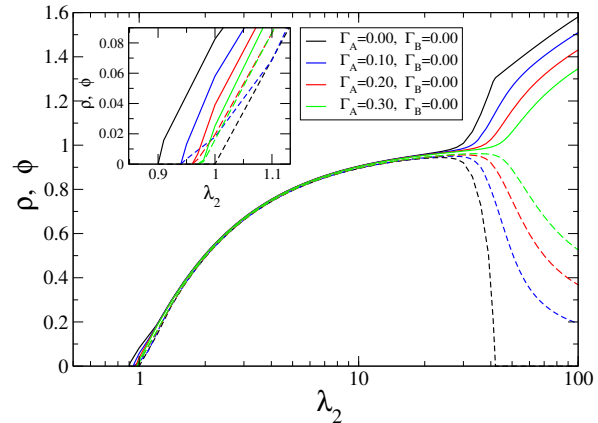


FIG. 3: Mean-field densities ϕ (solid curves) e ρ (dashed) for $\lambda_1 = 0.1$ and $\mu = 2.0$ with asymmetric disorder, $\Gamma_A \neq \Gamma_B$. Inset: detail of the data close to the absorbing transition (linear scale).

particle at one of its first neighbors with a probability $p_1 = \lambda_1/W$ or at one of its *second* neighbors with a probability $p_2 = \lambda_2/W$. Here, $W = (1 + \lambda_1 + \lambda_2 + \mu n_1^2)$ is the sum of the rates of all possible events. With a complementary probability $1 - (p_1 + p_2)$, the site is vacated. To improve the efficiency, we choose the sites from a list containing the currently N_{occ} occupied sites; accordingly, the time is incremented by $\Delta t = 1/N_{occ}$ after each event. For simulations in the subcritical and critical absorbing regime, we sample the quasi-stationary (QS) regime using the simulation method detailed in [29]. In order to draw a comparison with the results from MFT, in all cases we take $\mu = 2.0$.

B. Symmetric disorder

We begin by analysing the symmetric case, where $\Gamma_A = \Gamma_B = \Gamma$. In Fig. 4, we show typical configurations observed on the bipartite lattice for $\lambda_1 = 0.1$ and $\lambda_2 = 0.1$, for clean $\Gamma = 0$ and disordered system $\Gamma = 0.2$.

Figure 5 shows the densities of ρ and ϕ on a square lattice with linear system size $L = 80$. As expected, the absorbing phase transition occurs at a higher value of λ_2 when disorder is introduced. We also observe that increasing the fraction of disorder reduces the possibility of an AA phase, since the values of ϕ reduces when we increase the fraction of disorder.

In order to clarify the effects of disorder on the stability of the AA phase, we analyze the dependence of the order parameter ϕ with the linear system size L . In Fig. 6, we compare the clean model with the disordered system, with $\Gamma = 0.1$. Panels (a) and (b) show the order parameter ρ and ϕ versus λ_2 for distinct systems sizes. While for the clean version the the AA phase and the reentrant phase transition are observed for all system sizes (see

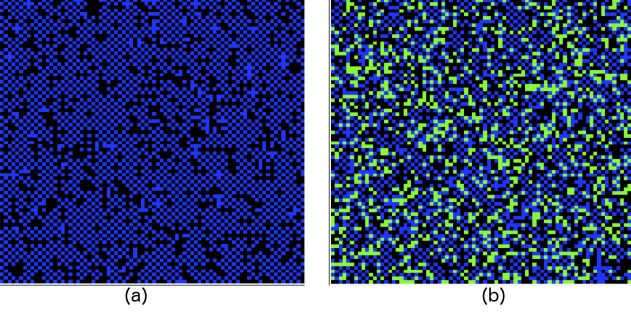


FIG. 4: (Color online) Typical configurations observed on the bipartite lattice for $\lambda_1 = 0.1$ and $\lambda_2 = 0.1$, for clean $\Gamma = 0.0$ and disordered system $\Gamma = 0.2$. Green: inert sites; Blue: occupied sites and Black: empty sites. Linear system size $L = 80$ and $\mu = 2.0$.

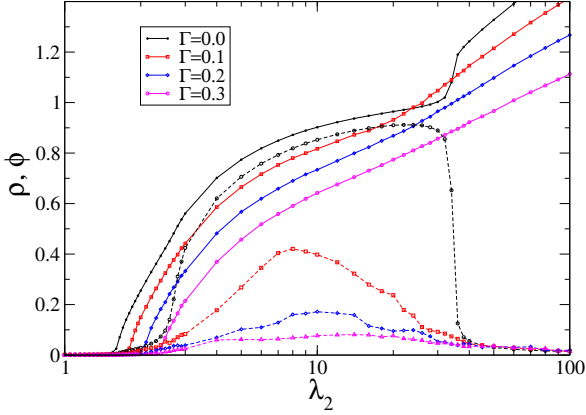


FIG. 5: Order-parameters ρ and ϕ for distinct (symmetric) Γ 's vs. λ_2 , for $\mu = 2$ and $\lambda_1 = 0.1$. Linear system size $L = 80$.

panel (a)), the disordered system shows a remarkably different picture, in which the sublattice occupations become equivalent for large L . Therefore, we conclude that ϕ vanishes when $L \rightarrow \infty$ and the AA phase is suppressed by the disorder. Such behavior is reinforced by analyzing the order parameter variance $\chi = L^2(\langle \phi^2 \rangle - \langle \phi \rangle^2)$, as shown in panels (c) (clean) and (d) (disordered). In contrast to the clean system, in which χ diverges nearby the transitions AB-AA and AA-AB as $L \rightarrow \infty$, no divergence is verified in such case. So, in contrast to the MFT predictions, we observe that symmetric disorder forbids the stability of AA phase and therefore the disordered system does not show symmetry breaking.

Now, let us characterize the absorbing phase transition in the disordered system. For locating the critical creation rate $\lambda_{2,c}$, we study the time evolution of the number of active particles $n(t)$ starting from an initial configuration the simulation with one pair of neighboring active particles. The critical value $\lambda_{2,c}$ can be estimated as the threshold λ_2 separating asymptotic growth from the decay towards the absorbing phase.

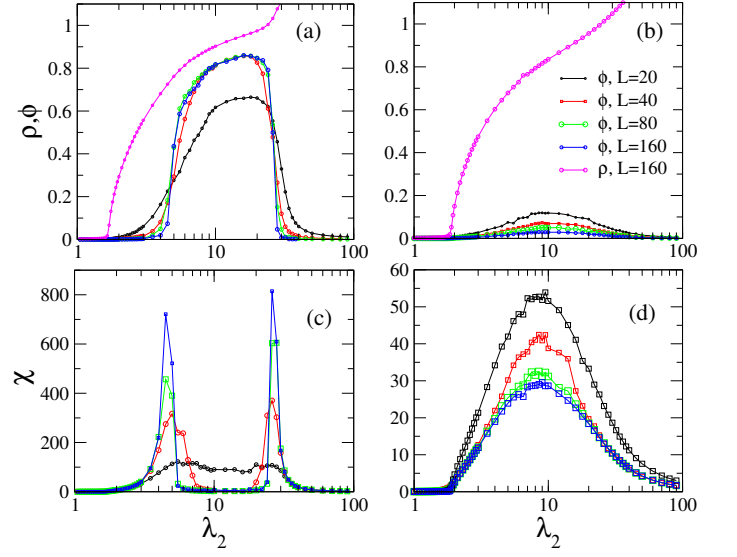


FIG. 6: Quasi-stationary densities ϕ and ρ vs. λ_2 , for $\mu = 2$ and $\lambda_1 = 0.1$, for the clean system (a), and for $\Gamma = 0.1$ (b). Scaled variance χ of the order parameter ϕ vs. λ_2 for $\mu = 2$ and $\lambda_1 = 0.1$, for the clean system (c), and for $\Gamma = 0.1$ (d).

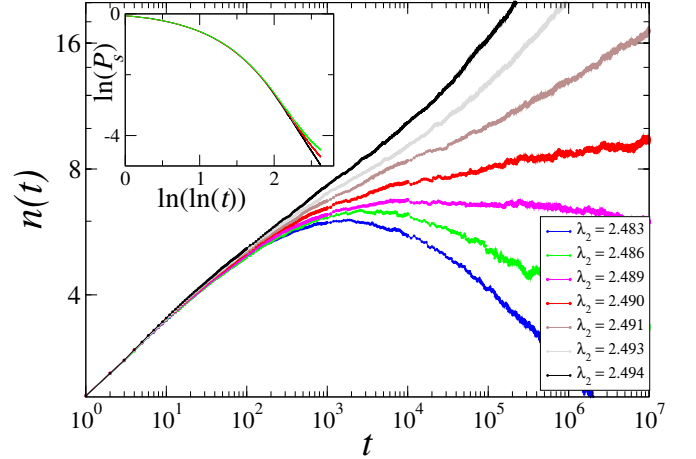


FIG. 7: Number of active particles n for $\Gamma = 0.3$, $\mu = 2$ and $\lambda_1 = 0.1$. Inset: survival probability for $\lambda_2 = 2.489$, 2.490 and 2.491 .

Figure 7 exemplifies the results for $\Gamma = 0.3$ in which $\lambda_{2,c} = 2.490(1)$. We observe that, analogously to the diluted CP, the critical behavior presents activated dynamic scaling, with

$$n(t) \sim \ln(t/t_0)^\theta \quad (5)$$

and with the survival probability

$$P_s \sim \ln(t/t_0)^{-\delta}. \quad (6)$$

From the data in Fig.7, we estimate $\ln(t_0) = 3.0(5)$, and $\theta = 0.21(4)$, in agreement with the value $\theta = 0.15(3)$, obtained in [24]. From the data shown in the inset of

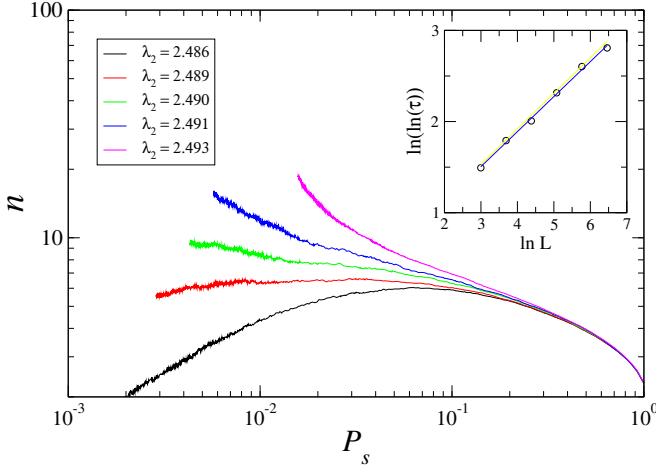


FIG. 8: . Log-log plot of the number of occupied sites n as a function of the survival probability P_s obtained from spreading simulations. Inset: Finite-size scaling of the lifetime of the QS state τ , for $\Gamma = 0.3$, $\mu = 2$ and $\lambda_1 = 0.1$.

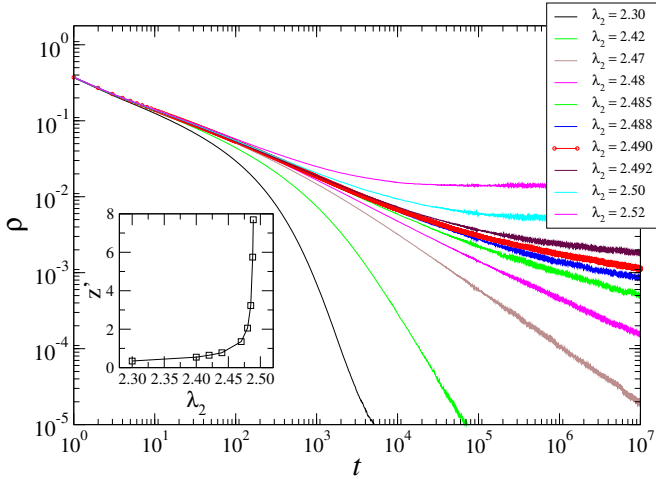


FIG. 9: Initial decay simulations: particle density ρ vs. t for $\mu = 2$ and $\lambda_1 = 0.1$ for symmetric disorder case, with $\Gamma = 0.3$ (linear system size $L = 2000$). Inset: Dynamical exponent z' as a function of λ_2 .

Fig. 7, we find $\delta = 2.1(3)$, very close to the value $\delta = 1.9(2)$ observed for the usual CP with random dilution, indicating that critical behavior of the disordered model belongs to the universality class of the diluted CP [24, 30].

Combining the activated scaling relations for $n(t)$ and $P_s(t)$, eqs. (5) and (6), we find that

$$n \sim P_s^{-\delta/\theta} \quad (7)$$

at criticality. This relation does not depend on t_0 , and is useful to check our estimate of the critical point. In Fig. 8, we plot n as function of P_s , and observe a power law that at $\lambda_2 = 2.490$, while the curves for $\lambda_2 = 2.491$ ($\lambda_2 = 2.489$) veers up (down), thus confirming the accuracy of our estimate for the critical point. At criticality, we found the exponent ratio $\delta/\theta = 0.09(2)$, in coherence with

the values of δ and θ obtained from the data in Fig. 7. This value is also in agreement with the value $\delta/\theta = 0.075(5)$ obtained for the diluted contact process in [30].

In the active-dynamical scenario, the lifetime of the process follows

$$\ln \tau \sim L^\psi, \quad (8)$$

where ψ is a universal exponent. From the data in the inset of Fig 8, we found $\psi = 0.44(5)$, close to the value $\psi = 0.51(6)$ obtained for the diluted CP [24].

Finally, another important effect that disorder can induce in absorbing phase transitions is the emergence of Griffiths phases. A Griffiths phase is a region inside the subcritical phase where the long-time decay of ρ towards the extinction is algebraic (with non-universal exponents), rather than exponential. In Fig. 9, we present results from initial decay simulations, where the system starts its dynamics from a fully occupied lattice. We observe the existence of a range of values of λ_2 in the subcritical regime where the long-time behavior of the density decays as a power law,

$$\rho(t) \sim t^{-2/z'} \quad (9)$$

with the non-universal dynamical exponents z' following

$$z' \sim |\lambda_2 - \lambda_{2,c}|^{-\psi\nu_\perp}, \quad (10)$$

where $\lambda_{2,c}$ is the critical value of the control parameter λ_2 [24]. In the inset of Fig. 9 we observe that z' diverges when λ_2 approaches $\lambda_{2,c} = 2.490$. From these data, we obtain $\psi\nu_\perp = 0.60(1)$, in good agreement with the value $\psi\nu_\perp \approx 0.61$ reported in [24] for the diluted CP.

In resume, our results for the effects of symmetric disorder are in agreement with the predictions from the Harris criterium, since $\nu_\perp = 0.734(4)$, for $d = 2$ in the clean system, and therefore the disorder is relevant for the absorbing phase transition [23]. Similar trends have been observed for lower values of Γ , although larger crossover times toward the infinite-random behavior are expected in such cases [23, 24].

C. Asymmetric disorder

Now, we investigate the effects of asymmetric disorder in which disorder strengths is different in each sublattice. This is exemplified in Fig. 10 for $\Gamma_1 = 0$ and distinct values of Γ_2 . We note that even a very small asymmetric disorder ($\Gamma_2 = 0.05$), the AS phase is suppressed and only less disordered sublattice is populated. Therefore, only a phase transition between the inactive and the asymmetric phase is presented, whose critical behavior is ruled by the less disordered sublattice. In all these cases, we observe that at criticality, $\rho \sim L^{-\beta/\nu_\perp}$ and the lifetime $\tau \sim L^{-z}$. For example, for $\Gamma_2 = 0.2$, shown in Fig 11, we find $\beta/\nu_\perp = 0.81(2)$ and $z = 1.75(3)$, in agreement with the DP values $\beta/\nu_\perp = 0.797(3)$ and $z = 1.7674(6)$. The

inset shows the moment ratios of the order parameter, $m = \langle \rho \rangle^2 / \langle \rho^2 \rangle$ goes to a universal value $m = 1.33(1)$ at criticality, in comparison to the known DP value $m = 1.3264(5)$ [13].

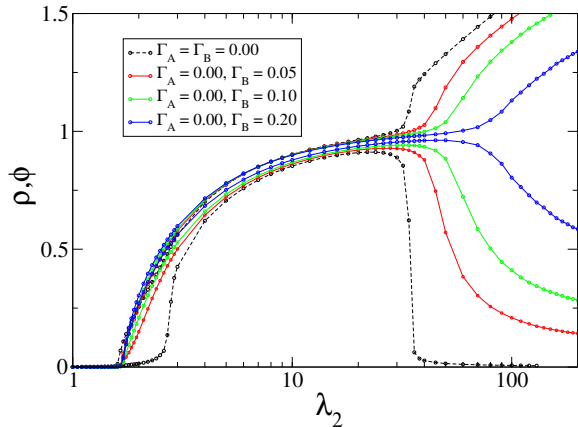


FIG. 10: For $L = 80$ and asymmetric disorder: Order-parameters ϕ and ρ for $\mu = 2$ and $\lambda_1 = 0.1$ for distinct Γ_A and Γ_B .

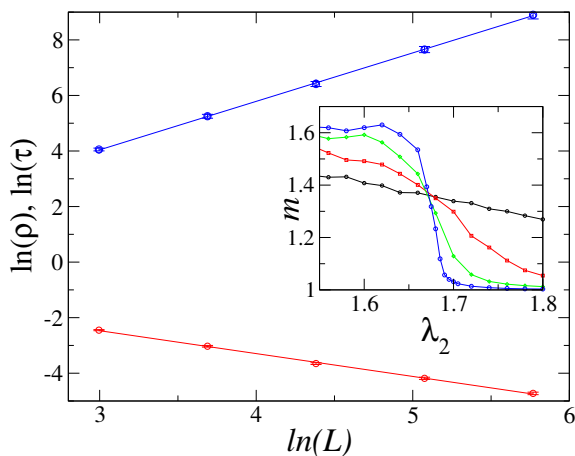


FIG. 11: Asymmetric disorder, with $\Gamma_1 = 0.0$ and $\Gamma_2 = 0.2$: Scaled critical QS density of active sites $\ln \rho$ (bottom) and scaled lifetime of the QS state $\ln \tau$ (top), versus $\ln L$. Inset: Moment ratio m versus λ_2 on a square lattice. Parameters: $\mu = 2$ and $\lambda_1 = 0.1$

D. Phase diagrams

Our simulation results for the effects of disorder are resumed in the phase diagrams shown in Fig.12. In (a), the clean system exhibits, besides the absorbing phase, a reentrant active asymmetric phase (with $\phi > 0$) inside

the active symmetric phase. In [13], it was shown that the active-absorbing phase belongs to the DP universality class, while the AA-AS symmetry-breaking phase transition is Ising-like.

The effects of asymmetric disorder in the phase diagram are shown in Fig.12 (b) and (c). We note that the AS phase vanishes, and there are only two phases, the absorbing and the AA phase. The universality class of the transition between these phases is governed by the less disordered sublattice. So, while in the case (b), the phase transition belongs to the DP universality class, in the case (c) it belongs to the universality class of the diluted CP.

Finally, if the disorder is symmetric, as in case (d), we note that the AA phase vanishes, and the absorbing-AS phase transition belongs to the class of the diluted CP. This system exhibits activated scaling and Griffiths phases as shown in detail in section III.B.

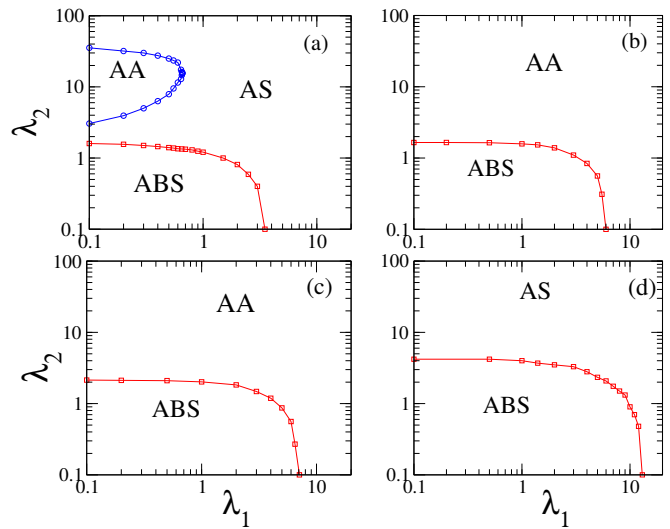


FIG. 12: Phase diagrams for (a) clean system, (b) $\Gamma_A = 0$ and $\Gamma_B = 0.3$, (c) $\Gamma_A = 0.1$ and $\Gamma_B = 0.3$, and (d) $\Gamma_A = \Gamma_B = 0.3$ ($\mu = 2$ in all cases).

IV. CONCLUSIONS

In this work, we have investigated the effects of quenched disorder in the phase diagram of the competitive contact processes on sublattices. Through mean-field analysis and Monte Carlo simulations, we have studied distinct types of disorder, (i) a random *homogeneous* deletion of sites (ii) an asymmetrical disorder, in which the disorder strength is different in each sublattice. Interesting, each one of the above disorder prescriptions yields completely different outcomes.

We observe that in the case (i), the disorder destroys the asymmetric active phase, and therefore, the symmetry-breaking phase transition. So, there are only two phases, the absorbing and the active (symmetric)

phases. The absorbing-active phase transition exhibited belongs to the universality class of the disordered contact process. Effects related to an infinite randomness fixed point are observed, such as activated dynamics and Griffiths phases in the subcritical regime.

A distinct behavior is observed if each sublattice has a different disorder strength. In such case, the symmetrical active phase is not stable, and we observe a phase transition directly from the active asymmetric phase to the absorbing phase. The critical behavior in this case is governed by the sublattice with less disorder, for instance, if one of the sublattices has no disorder, then the phase transition will fall in the DP class.

A natural extension of the present work would be the study of the effects of temporal disorder [31–34] on the robustness of the symmetry-breaking phase transition,

and in its the critical behavior. It is important to mention that, besides the theoretical interest in the field of nonequilibrium phase transitions, suppression of activity at the nearest neighbors of active sites resembles biological lateral inhibition, known to be important in the visual system of many animals [35]. Also, our work can be useful to understand the effects of heterogeneities in extended systems showing *checkerboard* pattern distributions such as mutually exclusive species co-occurrences [36].

Acknowledgments

This work was supported by CNPq and FAPEMIG, Brazil.

-
- [1] J. Marro and R. Dickman, *Nonequilibrium Phase Transitions in Lattice Models* (Cambridge University Press, Cambridge, 1999).
 - [2] H. Hinrichsen, Adv. Phys. **49**, 815 (2000).
 - [3] M. Henkel, H. Hinrichsen and S. Lubeck, *Non-Equilibrium Phase Transitions Volume I: Absorbing Phase Transitions* (Springer-Verlag, The Netherlands, 2008).
 - [4] G. Ódor, Rev. Mod. Phys. **76**, 663 (2004).
 - [5] K. A. Takeuchi, M. Kuroda, H. Chaté, and M. Sano, Phys. Rev. Lett. **99**, 234503 (2007).
 - [6] L. Corté, P. M. Chaikin, J. P. Gollub, and D. J. Pine, Nature Physics **4**, 420 (2008).
 - [7] S. Okuma, Y. Tsugawa, and A. Motohashi, Phys. Rev. B **83**, 012503 (2011).
 - [8] R. Gutiérrez, C. Simonelli, M. Archimi, F. Castellucci, E. Arimondo, D. Ciampini, M. Marcuzzi, I. Lesanovsky, and O. Morsch Phys. Rev. A **96**, 041602(R) (2017).
 - [9] N. Goldenfeld, *Lectures on phase transitions and the renormalization group* (Addison-Wesley, 1992).
 - [10] H. K. Janssen, Z. Phys. B **42**, 151 (1981); P. Grassberger, Z. Phys. B **47**, 365 (1982).
 - [11] I. Dornic, H. Chaté, J. Chave and H. Hinrichsen, Phys. Rev. Lett. **87**, 045701 (2001).
 - [12] M. J. de Oliveira, J. Stat. Phys. **66**, 273 (1992).
 - [13] M. M. de Oliveira and R. Dickman, Phys. Rev. E **84**, 011125 (2011).
 - [14] S. Pianegonda and C. E. Fiore, J. Stat. Mech. **2014**, P05008 (2014).
 - [15] M. M. de Oliveira and C. E. Fiore, J. Stat. Mech. **2017**, P053211 (2017).
 - [16] H. Hinrichsen, Braz. J. Phys. **30**, 69 (2000).
 - [17] A. J. Noest, Phys. Rev. Lett. **57**, 90 (1986).
 - [18] Moreira A G and Dickman R, Phys. Rev. E **54** R3090 (1996); Dickman R and Moreira A G, Phys. Rev. E **57** 1263 (1998).
 - [19] T. Vojta and M. Y. Lee, Phys. Rev. Lett. **96**, 035701 (2006).
 - [20] M. Bramson, R Durrett, and R. Schonmann, Ann. Prob. **19**, 960 (1991).
 - [21] M. S. Faria, D. J. Ribeiro and S. A. Salinas, J. Stat. Mech. P01022 (2008).
 - [22] A. B. Harris, J. Phys. C **7**, 1671 (1974).
 - [23] M. M. de Oliveira and S. C. Ferreira, J. Stat. Mech. P11001 (2008).
 - [24] T. Vojta, A. Farquhar and M. Mast, Phys. Rev. E **79**, 011111 (2009).
 - [25] M. M. de Oliveira, S.G. Alves, S.C. Ferreira and R. Dickman, Phys. Rev. E **78**, 031133 (2008).
 - [26] H. Barghathi and T. Vojta Phys. Rev. Lett. **113**, 120602 (2014).
 - [27] M. M. de Oliveira, S.G. Alves and S.C. Ferreira, Phys. Rev. E **93**, 012110 (2016).
 - [28] P.H.L. Martins and J.A. Plascak, Phys. Rev. E **76**, 012102 (2007).
 - [29] M. M. de Oliveira and R. Dickman, Phys. Rev. E **71**, 016129 (2005); M. M. de Oliveira and R. Dickman, Braz. J. Phys. **36**, 685 (2006).
 - [30] A. O Hada and M. J. de Oliveira, J. Stat. Mech. **2017**, 043209 (2017).
 - [31] F. Vazquez, J. A. Bonachela, C. López and M. A. Muñoz, Phys. Rev. Lett. **106**, 235702 (2011).
 - [32] R. Martínez-García, F. Vazquez, C. López, and M. A. Muñoz, Phys. Rev. E **85**, 051125 (2012).
 - [33] M.M. de Oliveira and C.E. Fiore, Phys. Rev. E **94**, 052138 (2016).
 - [34] C.E. Fiore, M.M. de Oliveira and J.A. Hoyos, Phys. Rev. E **98**, 032129 (2018).
 - [35] W. Lyttton, From Computer to Brain (Springer-Verlag, New York, 2002).
 - [36] E.F. Connor, M.D. Collins and D. Simberloff, Ecology **94**, 2403 (2013).